Kasetsart J. (Nat. Sci.) 49 : 1036 - 1046 (2015)

Monte Carlo Cellular Automata Simulation of Receptor Trafficking in Cell Signal Transduction: Tracking Dimer and Oligomer Formation

Chontita Rattanakul[1,2] and Yongwimon Lenbury[1,2,*]

ABSTRACT

A cellular automata (CA) model of the signal transduction pathway mediated by calcium sensing (CaS) receptors was constructed to investigate the effects of different fractions of healthy (functional) and defective receptors. Receptor trafficking was allowed to take place leading to dimerization and oligomerization which exerted a positive impact on the receptor binding affinity. Snapshots of receptor trafficking and distribution over the cell membrane simulated by the CA model were compared with the no-trafficking case.

Keywords: signal transduction, cellular automata, receptor trafficking, dimerization

INTRODUCTION

All living cells need to sense and respond to their environment. The common feature in all signal transduction pathways is that a component in the environment is recognized, typically by a protein in the plasma membrane (the receptor) and the environmental trigger is performed by the ligand where the receptor usually spans the membrane, and through binding to the ligand, triggers a change that activates an intracellular response termed signal transduction (Zito, 2009).

After a signal transduction pathway has been initiated and the information has been transduced to affect downstream cellular activities, the transduction process must be terminated. If termination is defective, cells lose their responsiveness to new signals, which can lead to uncontrolled cell growth and the possibility of cancer (Brennan *et al.*, 2013).

As has been observed by Mendes (2012), "several signal transduction pathways have been reported to be altered in cancer, leading to dramatic changes in cell survival, cell proliferation, morphology, angiogenesis, longevity and other properties, which characterize cancer cells." Also, faulty re-adjustments of the circulating calcium level, and consequently abnormalities in the insulin secretion mechanism can possibly be the result of defects in the signaling process involving the calcium-sensing (CaS) receptors (Kurbel *et al*., 1997).

According to several investigators (Bohen, 1995; Osuga *et al*., 1997), the defects in the signaling process may arise from many possible events; there may be an insufficient amount of functional CaS receptors expressed on the cell membrane that can efficiently bind with the ligand; the necessary dimerization process may

1 Department of Mathematics, Faculty of Science, Mahidol University, Bangkok 10400, Thailand.
2 Centre of Excellence in Mathematics, CHE, 328 Si Ayutthaya Road, Bangkok 10400, Thailand.
* Corresponding author, e-mail: scylb@yahoo.com

Received date : 02/04/15 Accepted date : 03/11/15

not be operating effectively in response to external stimuli such as hormone or drug intake; or ligand binding may be too transient, that is, receptor-ligand complexes are not sufficiently long-lived.

Wu *et al*. (2009) described how receptors such as the vascular endothelial growth factor (VEGF) receptors and other members of the same family, require dimerization in order to become active. Before the receptor monomers bind with VEGF, they diffuse throughout the cell membrane as singletons or as "ligand-independent pre-associated dimmers" (Wu *et al*., 2009).

This paper presents the simulation results of a CA model of signal transduction pathway mediated by CaS receptors, that was constructed to investigate the effects that receptor dimerization and oligomerization have on receptor binding affinity. The receptor population can be divided into groups of healthy (functional) and defective receptors which behave differently in terms of receptor affinity, longevity and trafficking over the cell membrane. Snapshots of the simulations were taken to compare the receptor distribution on the membrane and dimer formation where trafficking is assumed to take place with the case where trafficking is not incorporated.

CELLULAR AUTOMATA MODEL

CA model simulation was performed in MATLAB and averaged over 10 runs for each configuration. Experimentation with additional runs resulted in no difference in the the average so that more runs were considered to be unnecessary. The CA model is defined on a square lattice of size S x S, using Moore's neighborhood with a range of 1 (Jørgensen *et al.*, 2009). The states of the cells in the lattices are updated at each time step in parallel according to given rules, with each time step corresponding to 3 s.

Apart from being an empty space, each site on the lattice is occupied by a receptor which is assigned one of the eight states that describe the possible states in which those receptors may be found at time step t. These are defined in Table 1.

Coupled to the CA model, the concentrations of cytosolic and extracellular free Ca^{2+} were computed using a system of difference equations. These calcium levels in turn exert feedback and feed-forward effects on the receptor binding affinity and longevity. The calcium levels are updated every time step, and the new levels are used in the update rules for the receptor binding.

The intracellular calcium concentration I_t and extracellular calcium concentration E_t at any time t are updated according to Equations 1 and 2, respectively:

$$I_{t+\Delta t} - I_t = \alpha BH_t + \beta B1_t + \gamma B2_t - \frac{K_F K_{dF} I_t}{K_{dF} + I_t} - \frac{K_B K_{dB} I_t}{K_{dB} + I_t} - \varepsilon\left(I_t - s\left(E_t + E_e\right)\right) + \delta \quad (1)$$

$$E_{t+\Delta t} - E_t = \varepsilon\left(I_t - s\left(E_t + E_e\right)\right) - \varpi E_t \quad (2)$$

Table 1 Definitions of state variables.

Symbol	Definition	Symbol	Definition
N_t	Non-activated receptors at time t	H_t	Activated free healthy receptors which function normally at time t
BH_t	Ligand-bound healthy receptors		
$F1_t$	Defective or faulty activated free receptors type I that exhibit less binding affinity than H_t and have shorter half-life or less long-lived at time t	$F2_t$	Activated faulty free receptors type II which dissociate immediately after binding to the ligand at time t
$B1_t$	Ligand-bound faulty receptors type one at time t	$B2_t$	Ligand-bound faulty receptors type two at time t

where ε is the rate constant of calcium efflux from intracellular compartment (Jirounek, 1988), $s = 1 \times 10^4$ is the scaling factor between the intracellular and extracellular compartments, δ is the production rate independent of CaS receptors or other binding effects, ϖ is the removal rate of extracellular calcium, whereas α, β and γ are the calcium production rate constants due to the levels of healthy receptors, faulty receptors types 1 and 2, respectively, E_e is the extracellular calcium concentration at equilibrium and Δt corresponds to one time step which is 3 s in the simulations.

The fourth term in Equation 1 models the binding of calcium by the endogenous cellular buffers, whereas the fifth term models the binding of calcium by fura-2. As calcium diffuses through the cell body, it can be bound by both the buffers and the fura-2. Here, K_F is the calcium binding rate constant and K_{dF} is the fura binding saturation constant, whereas K_B is the calcium buffering rate constant and K_{dB} is the corresponding buffering saturation constant. These terms have been derived by following the work of Blumenfeld *et al*. (1992). In Equation 2, ϖ is the efflux rate from the extracellular compartment (Blumenfeld *et al*., 1992).

In each time step, all sites (*i, j*) are updated by first updating all the non-activated receptors at random, then all types of ligand-bound receptors next at random, then the rest of the sites are updated at random. If the randomized cell is empty, no change occurs.

For each site (*i,j*), a distant neighborhood can be any of the sites ($i \pm 2, j \pm k$), $k = 0,1,2$, or ($i \pm k, j \pm 2$), $k = 0,1$. A far distant neighborhood can be any of the sites ($i \pm 3, j \pm k$), $k = 0,1,2,3$, or ($i \pm k, j \pm 3$), $k = 0,1,2$.

At each time step, a number r, $0 \le r \le 1$, is randomized. The flowchart of the main routine to update all cells in the lattice is given in Figure 1. Here, loop D is the update of non-activated receptors *N*, and is shown in Figure 2. It is assumed here that the total concentration of ligand [L] is present at a constant abundant amount.

The healthy free receptor H_t may bind to ligand becoming a healthy bound receptor BH_t if $r > r_3$, where $r_3 = e^{-(k_2[L]+k_3 I_t)}\left(1 - e^{-k_4 E_t}\right)$. If $r \le r_3$ and it has at least one bound receptor in its neighborhood, it may become a BH_t forming a dimer if $r_3 r_4 < r \le r_3$. If $r \le r_3$ and it does not have any bound receptor in its neighborhood, but has a bound receptor in its distant neighborhoods, it may move towards a bound receptor in its distant neighborhoods (randomized if there are more than one) provided $r_3 r_5 < r \le r_3$ to become bound, forming a dimer.

If $r \le r_3$ and it does not have any bound receptor in its neighborhood or distant neighborhoods, but has a bound receptor in its far distant neighborhoods, it may move to its immediate neighborhood cell closer to a bound receptor in its far distant neighborhoods (randomized if there are more than one) provided $r_3 r_5 < r \le r_3$. Otherwise, it remains unchanged. The movements of these receptors toward a neighboring receptor are assumed to take place under the rule of the shortest possible distance traveled.

The free faulty receptor of type 1 *F1* can bind to the ligand in the same manner as the healthy receptors, but with a lower binding affinity, r_6 instead of r_3, $r_6 = \rho_1 r_3$, $\rho_1 < 1$ and r_7 instead of r_4, $r_7 = \rho_2 r_4$, $\rho_2 > 1$. They are also able to move and form dimers with other coupled receptors with the same trafficking rules. The free faulty receptors of type 2 *F2* can bind to the ligand in the same manner as the healthy receptors, but with an even lower binding affinity, r_8 instead of r_3, $r_8 = \rho_3 r_3$, $\rho_1 < 1$ and r_9 instead of r_4, $r_9 = \rho_4 r_4$, $\rho_4 > \rho_2 > 1$. They are also able to move and form dimers with other coupled receptors with the same trafficking rules. The flowchart for the updates of bound healthy receptors BH_t is given in Figure 3a where each has a life span τ_h. It could dissociate at the probability r_{10}, where $r_{10} = \left(1 - e^{-k_{-1}}\right)e^{-k_5 C_t^i}$. It dissociates back into a non-activated receptor *N* at the probability $r_{10} r_{11}$, $r_{11} = 1 - e^{-k_r}$. Otherwise it dissociates into a healthy free receptor.

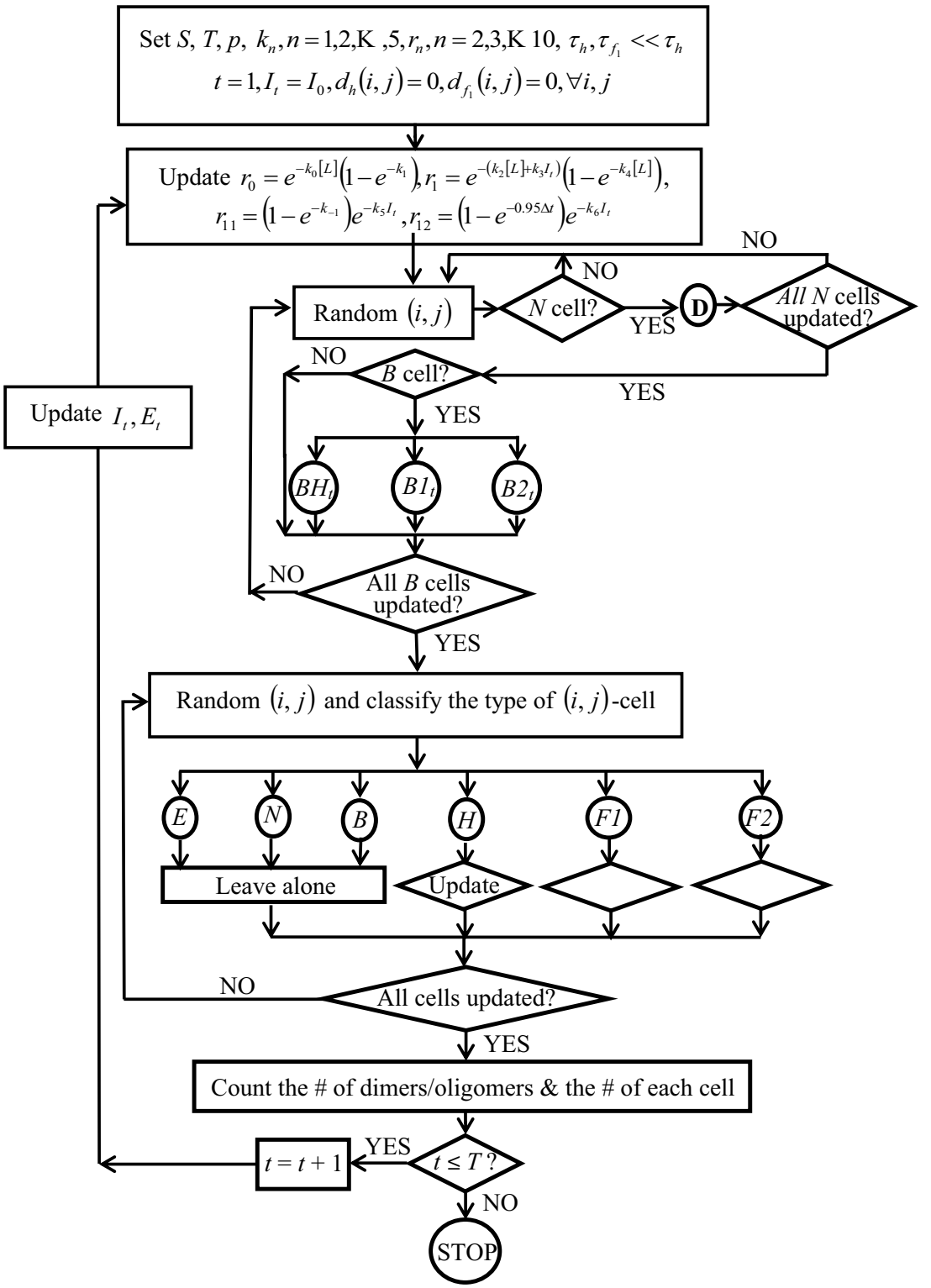


Figure 1 Flowchart of the main routine.

The bound faulty receptors of type 1 are updated in a similar manner as the bound healthy receptors but with shorter life span τ_{f1}. It could dissociate at the probability r_{12}, where $r_{12} = \left(1 - e^{-0.95\Delta t}\right) e^{-k_6 C_t^i} > r_{10}$. It dissociates back into a non-activated receptor N at the probability $r_{11} r_{12}$. Otherwise it dissociates into a faulty receptor $F1$. Finally, the flowchart for the update of bound faulty receptors of type 2 is given in Figure 3b.

RESULTS

The snapshots of the CA simulations are shown in Figures 4 and 5. The values and the meanings of the parameters used in the simulations are given in Table 2.

These parameters have been estimated based on the figures and rates of change reported in the literature (Bell, 1978; Gambhir *et al*., 1978; Ciechanover *et al*., 1983; Stoscheck and Carpenter, 1984; Jirounek *et al*., 1988; Bajzer *et al*., 1989; Blumenfeld *et al*., 1992; Postma and Van Haastert, 2001; Zito, 2009; Gibbons *et al*., 2010; Conrad, 2014; Romm, 2014). The rates of change have been converted to probabilities using the standard conversion formula described by Myriam Hunink *et al*. (2001).

In Figure 4, the receptors are allowed to move towards bound receptors leading to higher binding affinity. In Figure 5, no trafficking is allowed. It can be observed that less clusters are formed when receptors do not move and, as a result, receptors bind to ligands more slowly. In the same amount of time, there appear more bound receptors (pink and yellow) and they are more clustered together in the trafficking case (Figure 4) than in Figure 5.

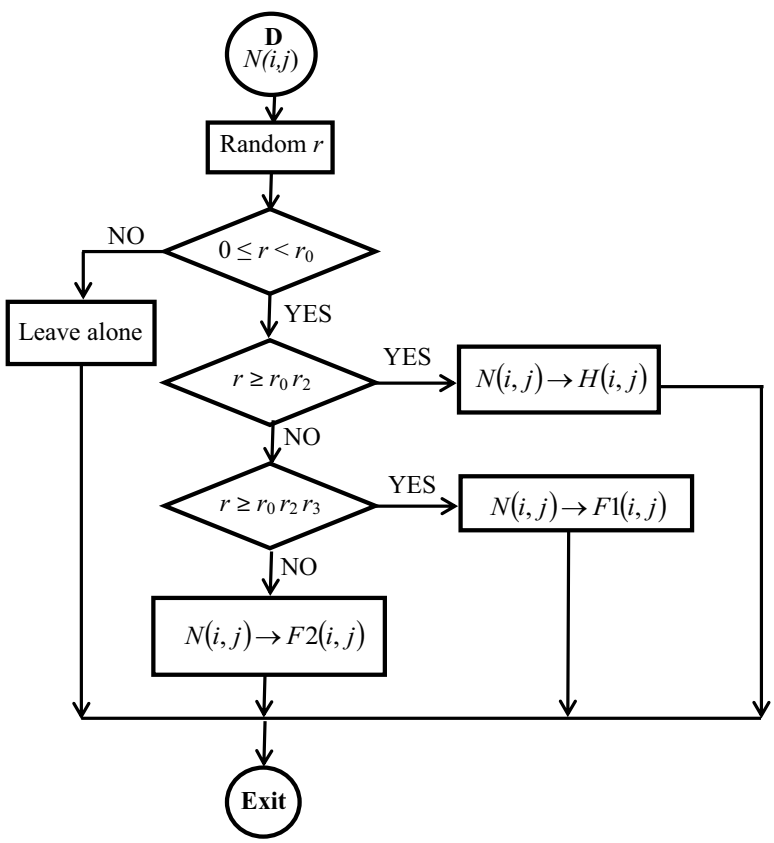


Figure 2 Flowchart of loop D to update the non-activated receptors N_t in the (i, j) location.

Figure 6 shows the development of clusters of receptors seen to grow in size but decrease in number. The number of dimers/ oligomers with trafficking is compared with that without trafficking in Figures 7a and 7b. The graphs have been obtained by averaging over 10 simulation runs in the same construction. Since the simulated curves from different runs appear very close to each other, it was not necessary to average a higher number of runs that what is presented here.

It was observed that the curve of the number of clusters in the no-trafficking case remained below the curve when trafficking takes place. However, as time progressed the numbers of bound receptors that formed themselves into clusters became closer to each other because almost all receptors eventually become bound, filling up almost the entire membrane surface. As more and more receptors form themselves into clusters, the number of clusters decreases as seen in Figure 7a.

There are no available experimental data on the number of dimers or oligomers in the literature, as far as is known. In order to verify that the CA model is a good representation of the process under investigation, the simulated time courses of calcium concentrations, shown in Figures 7c and 7d were compared with those reported by Tao *et al*. (1998) and Fridlyand

free receptor.

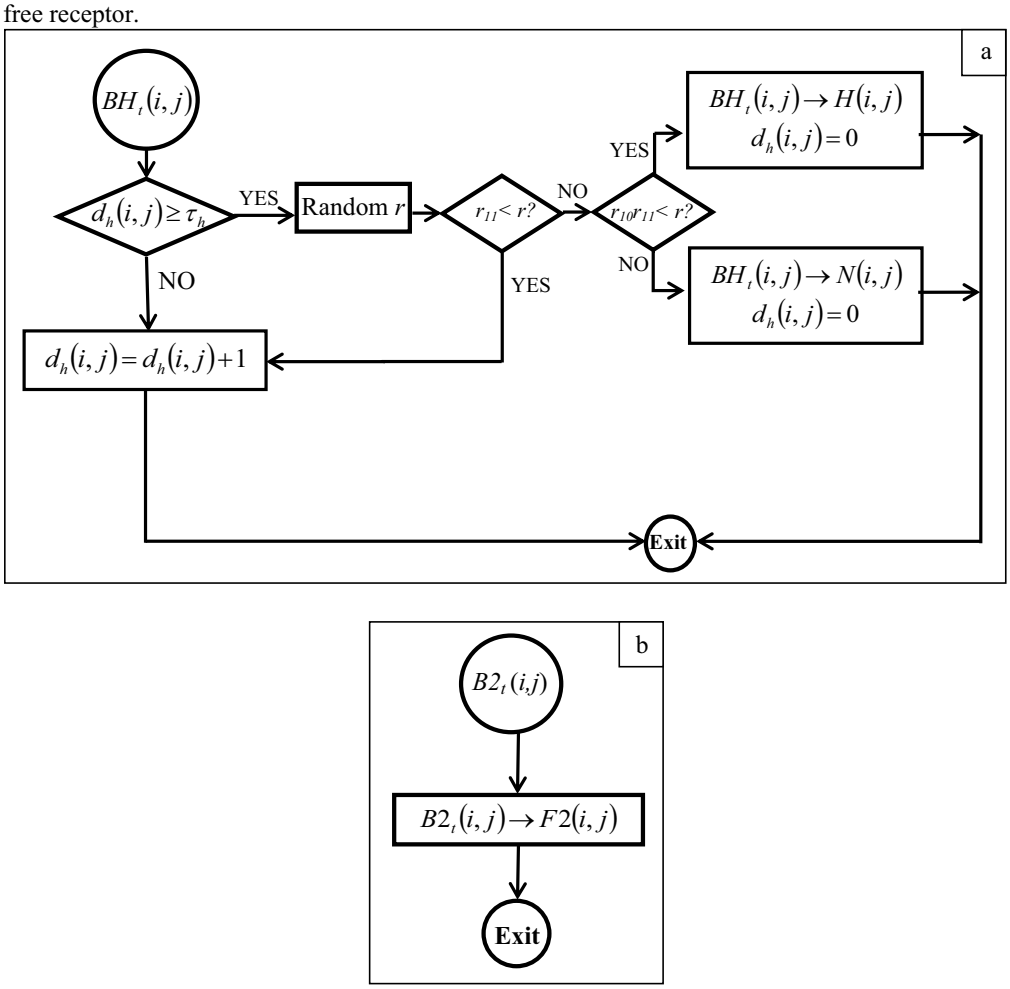


Figure 3 Updates of bound receptors that are (a) healthy and (b) faulty type 2.

et al. (2010), among many others, which exhibit oscillatory behavior closely resembling the results of the current simulations. Thus, the current model is able to reproduce various types of dynamic behavior observed in clinical settings using reasonable parameter values, some of which having been converted, as mentioned earlier, from the rate constants reported in the literature, whereas others have been estimated based on available information therein.

Table 2 Parameter values.

Symbol	Meaning	Value
S	Lattice dimension	120
$[L]$	Total concentration of ligand	9.4×10^{-11}
τ_h	Life span of bound healthy receptors	16 time steps
τ_{fl}	Life span of bound faulty receptors type 1	5 time steps
k_{-1}	BH_t dissociation rate constant	2.1
k_0	Constant for influence of E_t on receptor activation	3.5×10^{2}
$k_1=V_r$	Receptor activation rate	$2.24\Delta t$
$k_2=k_a$	Receptor binding rate	$1.6\times10^{7}\Delta t\ M^{-1}$
k_3	Constant for influence of I_t on receptor binding	1.0×10^{5}
k_4	Constant for influence of E_t on receptor binding	4.5×10^{3}
k_5	Constant for influence of I_t on bound healthy receptor dissociation	1,500
k_6	Constant for influence of I_t on bound faulty receptor dissociation	1,500
k_r	Receptor recycling rate constant	$1.3\times10^{-3}\Delta t$
r_1	Constant deciding whether N_t becomes an active healthy free receptor	0.56
r_2	Constant deciding whether N_t becomes an active faultyy free receptor	0.5
r_4	Probability H_t becomes BH_t if it has a BH_t in its distant neighborhood	0.2
r_5	Probability H_t becomes BH_t if it has a BH_t in its far distant neighborhood	0.01
ρ_1	Scaling factor to lower binding affinity of F_1 with BH_t in neighborhood	0.2
ρ_2	Scaling factor to lower binding affinity of F_1 with BH_t in distant neighborhood	2.0
ρ_3	Scaling factor to lower binding affinity of F_2 with BH_t in neighborhood	0.36
ρ_4	Scaling factor to lower binding affinity of F_2 with BH_t in distant neighborhood	3.0
K_F	Calcium binding rate constant	7.5×10^{-1}
K_{dF}	Fura binding saturation constant	7.6×10^{-7} mole litre^{-1}
K_B	Calcium buffering rate constant	6.0×10^{-1}
K_{dB}	Buffering saturation constant	5×10^{-6} mole litre^{-1}
E_e	Extracellular calcium concentration at equilibrium	0.002 mole/litre
α	Calcium production rate due to the healthy receptors	4.53×10^{-11}
β	Calcium production rate due to faulty receptors type 1	$e^{-20/100}\alpha$
γ	Calcium production rate due to the faulty receptors type 2	$e^{-36/100}\alpha$
δ	Zero order calcium production rate	1.36×10^{-11} mole litre^{-1}
ε	Rate of calcium efflux from intracellular compartment	$1.83\times10^{-3}\Delta t$
s	Scaling factor intracellular $\leftrightarrow$ extracellular compartments	10^{-4}
ϖ	Efflux rate from the extracellular compartment	$3.33\times10^{-3}\Delta t$

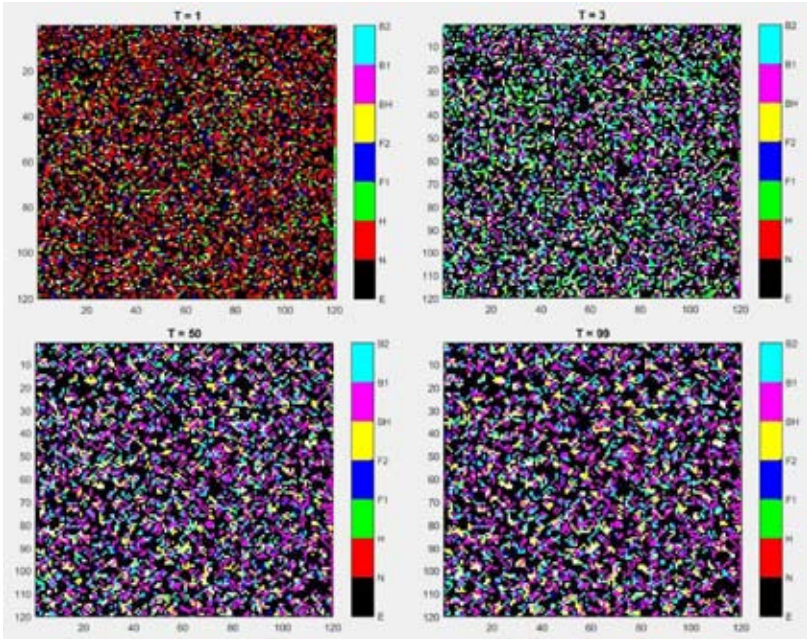


Figure 4 Snapshots of cellular automata simulation showing cell membrane distribution and transformation of different types of receptors with trafficking. Here, $F1_0 = F2_0 = 560$, $H_0 = 880$, $BH_0 = 240$, $B1_0 = B2_0 = 180$, $E_0 = 0.0005$ mole.L^{-1}, $E_e = 0.002$ mole.L^{-1}, $I_0 = 10^{-4} \times (E_0 + E_e)$, $\Delta t = 3$ s. The chosen parameters values are estimated based on the literature given in the text.

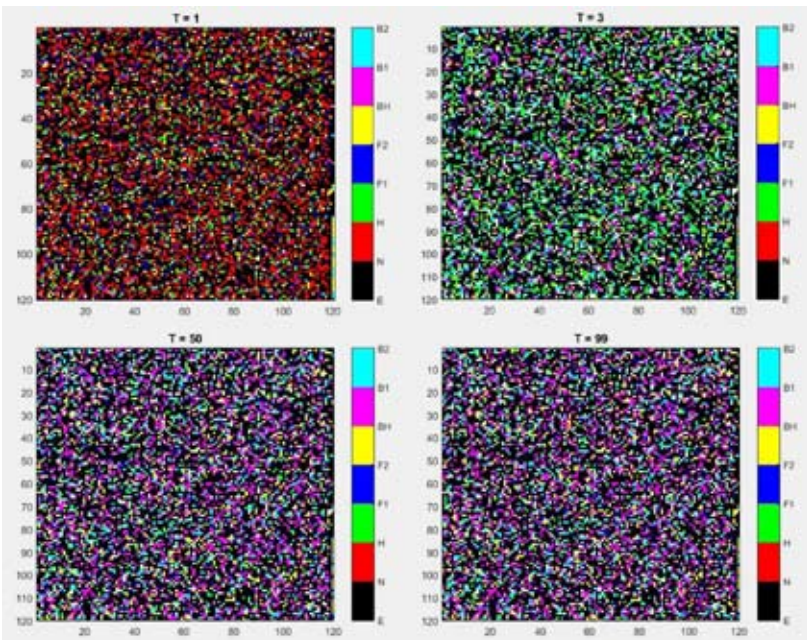


Figure 5 Snapshots of cellular automata simulation showing cell membrane distribution and transformation of different types of receptors with no trafficking. The parameter values are the same as in Figure 4 except r_4 is set equal to 1 so that trafficking does not take place.

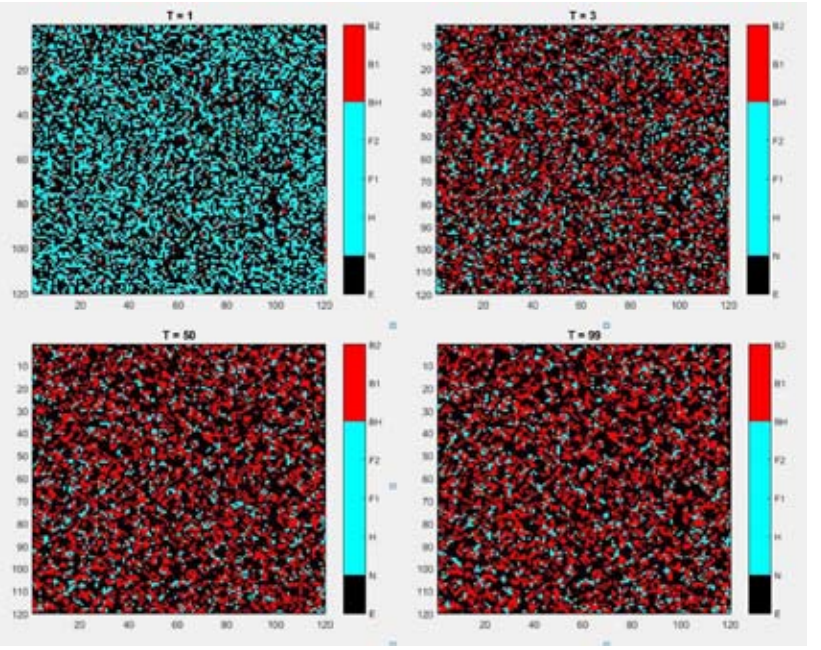


Figure 6 Clusters of bound receptors (in red) are seen to grow in size but decrease in number with trafficking. The same parametric values as in Figure 4 are used.

As mentioned earlier, the values of the parameters used in the simulations are given in the caption of Figure 4 These parameters have been estimated based on the figures and rates of change reported in the literature (Bell, 1978; Gambhir *et al*., 1978; Ciechanover *et al*., 1983; Stoscheck and Carpenter, 1984; Jirounek *et al*., 1988; Bajzer *et al*.,1989; Blumenfeld *et al*., 1992; Postma and Van Haastert, 2001; Zito, 2009; Gibbons *et al.*, 2010; Conrad, 2014; Romm, 2014). Several simulations were carried out using other sets of parameter values but it was found that the intracellular calcium concentration did not show as pronounced an oscillatory behavior which has often been observed in expermental data.

CONCLUSION

The impact of dimerization/oligomerization on CaS receptor binding and distribution on the cell membrane was investigated through the use of a cellular automata simulation technique. The effects were felt indirectly through the increase in binding affinity which led to a higher rate of production of bound receptors and, as a result, an elevated intracellular calcium concentration. In the present work, the direct effects of dimerization on the calcium dynamics have not been incorporated explicitly in their update equations. It is interesting to note that the number of receptor clusters simulated by the current model was observed to fluctuate quite randomly. The impact of such chaotic fluctuations in the number of receptor clusters on the kinetics of calcium should be of great interest, and hence a subject for future investigation, especially since keeping the level of circulating ionized calcium within a narrow physiological range is clearly essential for the human body to function properly.

ACKNOWLEDGEMENT

This research was supported by the Centre of Excellence in Mathematics, Commission on Higher Education, and Mahidol University, Bangkok, Thailand.

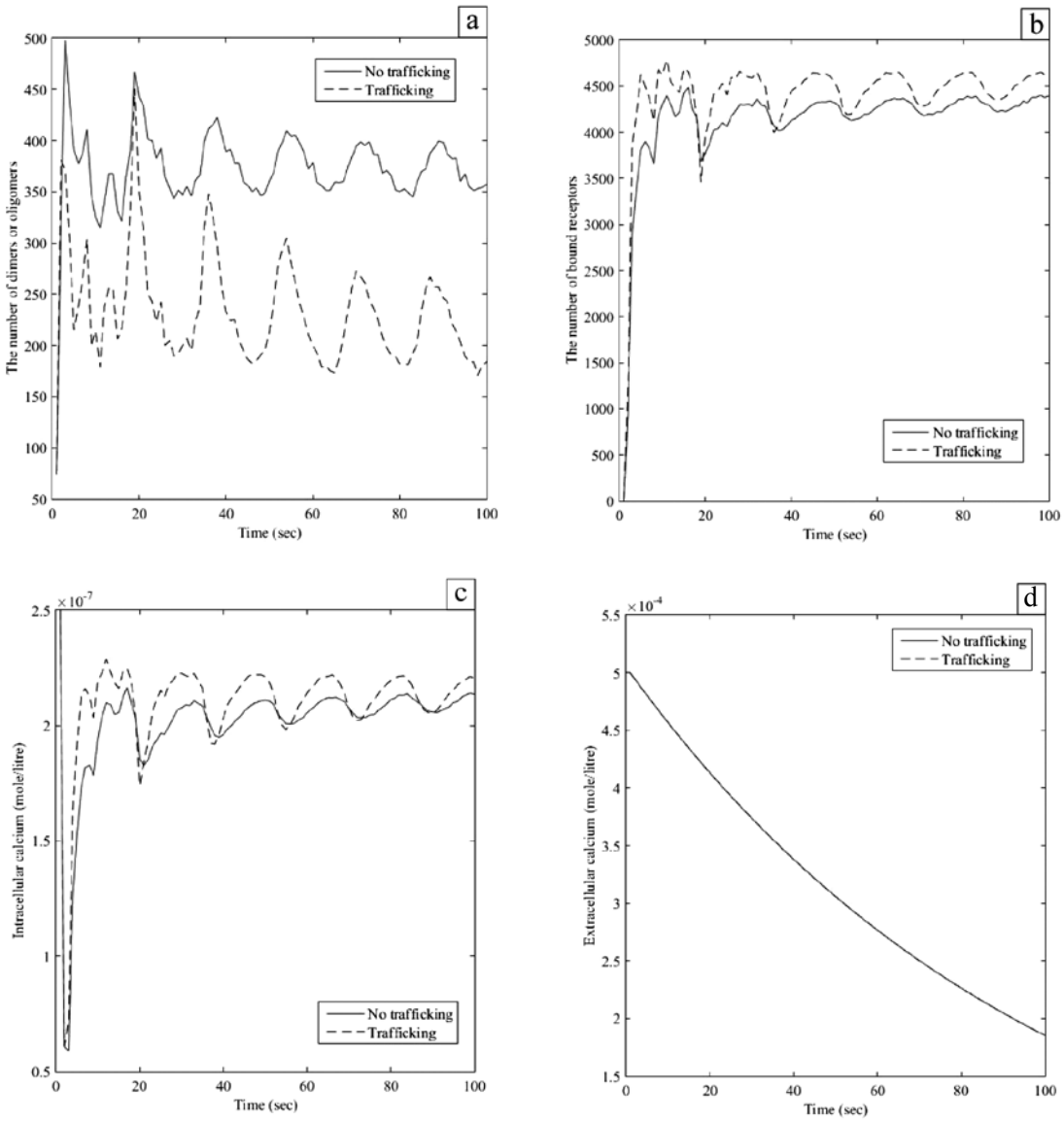


Figure 7 (a) Number of dimers or oligomers formed as time passes; (b) Number of bound receptors that form themselves into dimers or oligomers; (c) Intracellular calcium; (d) Extracellular calcium.

LITERATURE CITED

Bajzer, Z., A.C. Myers and S. Vuk-Pavlovii. 1989. Binding, internalization and intracellular processing of proteins interacting with recycling receptors Akindic analysis. **J. Biol. Chem.** 264: 13623–13631.

Bell, G.I. 1978. Models for the specific adhesion of cells to cells. **Science** 200: 618–627.

Blumenfeld, H., L. Zablow and B. Sabatin. 1992. Evaluation of cellular mechanisms for modulation of calcium transients using a mathematical model of fura-2 Ca" imaging in Aplysia sensory neurons. **Biophysics** 63: 1146–1164.

Bohen, S.P. 1995. Hsp90 mutants disrupt glucocorticoid receptor ligand binding and destabilize aporeceptor complexes. **J. Biol. Chem.** 270: 29433–29438.

Brennan, S.C., U. Thiem, S. Roth, A. Aggarwal, I.S. Fetahu, S. Tennakoon, A.R. Gomes, M.L. Brandi, F. Bruggeman, R. Mentaverri, D. Riccardi and E. Kallay. 2013. Calcium sensing receptor signalling in physiology and cancer. **Biochim. Biophys. Acta** 1833: 1732–1744.

Ciechanover, S.A., A.L. Schwartzgll, A. Dautry-Varsat and H.F. Lodish. 1983. Kinetics of internalization and recycling of Transferrin and the Transferrin receptor in a human Hepatoma cell line. **J. Biol. Chem.** 258: 9681–9689.

Conrad, D.R. 2014. **Calcium in cell culture.** [Available: http://www.sigmaaldrich.com/life-science/cell-culture/learning-center/media-expert/ calcium.html]. [Sourced: 25 May 2014].

Fridlyand, L.E., N. Tamarina and L.H. Philipson. 2010. Bursting and calcium oscillations in pancreatic β cells: Specific pacemakers for specific mechanisms. **Am. J. Physiol. Endocrinol. Metab.** 299: E517–E532.

Gambhir, K.K., J.A. Archer and C.J. Bradley. 1978. Characteristics of human erythrocyte insulin receptors. **Diabetes** 27: 701–708.

Gibbons, M.M., T. Chou and M.R. D'Orsogna. 2010. Diffusion-dependent mechanisms of receptor engagement and viral entry. **J. Phys. Chem. B** 114: 15403–15412.

Jirounek, P., J. Vitus, W.F. Pralong and R.W. Straub. 1988. Calcium efflux and intracellular exchangeable calcium in mammalian nonmyelinated nerve fibers. **J. Membr. Biol.** 103: 121–134.

Jørgensen, S.E., T-S. Chon and F. Recknagel 2009. **Handbook of Ecological Modelling and Informatics,** WIT Press. Southampton, UK

Kurbel, B., S. Kurbel, Z. Kristek, M. Jakić, M. Jurić and D. Sulava. 1997. Simulation model of defective insulin receptors as byproducts of receptor recycling. **Med. Hypotheses** 49: 165–70.

Mendes, R.A. R.A. 2012. Oncogenic pathways in the development of oral cancer. **J. Carcinog. Mutagen.** 3:133. doi:10.4172/2157-2518. 1000133.

Myriam Hunink, M.G., P.P. Glasziou, J.E. Siegel, J.C. Weeks, J.S. Pliskin, A.S. Elstein and M.C. Weinstein. 2001. **Decision Making in Health and Medicine: Integrating Evidence and Values,** Cambridge University Press. Cambridge, UK.

Osuga, Y., M. Hayashi, M. Kudo, M. Conti, B. Kobilka and A.J.W. Hsueh. 1997. Co-expression of defective Luteinizing hormone receptor fragments partially reconstitutes ligand-induced signal generation. **J. Biol. Chem.** 272: 25006–25012.

Postma, M. and P.J.M. Van Haastert. 2001. A diffusion-trans location model for gradient sensing by chemotactic cells. **Biophys. J.** 81: 1314–1323.

Romm, I. 2014. **Hormones-Receptors.** [Available: http://www.bumc.bu.edu/mybusm/files/2009/08/ endocrinology review.pdf]. [Sourced:9 Feb 2014].

Stoscheck, M.C. and G. Carpenter. 1984. Direct demonstration of receptor degradation in human fibroblasts. **J. Cell Biol.** 98: 1048–1053.

Tao, C., M. Yamamoto, H. Mieno, M. Inoue, T. Masujima and G. Kajiyama. 1998. Pepsinogen: coupling of exocytosis visualized by video microscopy and [Ca2+] in single cells. **Am. J. Physiol. Gastrointest. Liver. Physiol.** 274: G1166–G1177.

Wu, F.T., M.O. Stefanini, F. Mac Gabhann, C.D. Kontos, B.H. Annex and A.S. Popel. 2009. Computational kinetic model of VEGF trapping by soluble VEGF receptor-1: effects of transendothelial and lymphatic macromolecular transport. **Physiol. Genomics** 38: 29–41.

Zito., K. 2009. **NMDA receptor function and physiological modulation.** Elsevier Ltd. Amsterdam, the Netherlands.